



Modeling of new markers for the diagnosis and prognosis of pancreatic cancer based on the transition from inflammation to cancer

Yuan Zhou^{1,2,3#}, Borong Huang^{1,2,3#}, Qinqin Zhang⁴, Yaqun Yu³, Juan Xiao^{1,2}

¹Guangxi Key Laboratory of Molecular Medicine in Liver Injury and Repair, Affiliated Hospital of Guilin Medical University, Guilin, China;

²Guangxi Health Commission Key Laboratory of Basic Research in Sphingolipid Metabolism Related Diseases, Affiliated Hospital of Guilin Medical University, Guilin, China; ³Department of Hepatobiliary and Pancreatic Surgery, Affiliated Hospital of Guilin Medical University, Guilin, China;

⁴Department of Thyroid and Breast Surgery, Nanxishan Hospital of Guangxi Zhuang Autonomous Region, Guilin, China

Contributions: (I) Conception and design: J Xiao; (II) Administrative support: J Xiao, Y Yu; (III) Provision of study materials or patients: J Xiao; (IV) Collection and assembly of data: Y Zhou; (V) Data analysis and interpretation: Y Zhou, B Huang; (VI) Manuscript writing: All authors; (VII) Final approval of manuscript: All authors.

[#]These authors contributed equally to this work.

Correspondence to: Juan Xiao, PhD. Guangxi Key Laboratory of Molecular Medicine in Liver Injury and Repair, Affiliated Hospital of Guilin Medical University, No. 15, Lequn Road, Xiufeng District, Guilin 541001, China; Guangxi Health Commission Key Laboratory of Basic Research in Sphingolipid Metabolism Related Diseases, Affiliated Hospital of Guilin Medical University, Guilin, China. Email: xj042386@sina.com or xiaojuan@glmc.edu.cn; Yaqun Yu, MD. Department of Hepatobiliary and Pancreatic Surgery, Affiliated Hospital of Guilin Medical University, No. 15, Lequn Road, Xiufeng District, Guilin 541001, China. Email: yyq0129@glmc.edu.cn.

Background: Pancreatic adenocarcinoma (PAAD) is a lethal disease with a poor prognosis. Genes involved in acute pancreatitis (AP) or chronic pancreatitis (CP) might be important for PAAD development. This study sought to identify potential PAAD diagnosis markers and to establish a PAAD prognosis prediction model based on AP- and CP-related genes.

Methods: The significantly differentially expressed genes in both AP or CP and PAAD were obtained by a bioinformatics analysis. A risk-score model for predicting survival was constructed based on The Cancer Genome Atlas (TCGA) data and validated using an International Cancer Genome Consortium (ICGC) cohort. Protein expression and the effects of the genes in the risk models were validated by immunohistochemistry, or Cell Counting Kit-8 (CCK-8) and transwell assays. The study sample data included six AP tissue samples and five normal pancreatic tissue samples, six CP tissue samples and six normal pancreatic tissue samples from the Gene Expression Omnibus (GEO) expression profiling microarrays GSE109227 and GSE41418 data sets, respectively, and fragments per kilobase per million mapped fragments (FPKM) data from four normal controls and 150 PAAD cases from TCGA database, and 182 cancer patient samples with complete survival prognostic data from the ICGC database.

Results: In total, 508 significantly differentially expressed genes were found in both AP or CP and PAAD. Trefoil factor 2 (*TFF2*), tubulointerstitial nephritis antigen (*TINAG*), trefoil factor 1 (*TFF1*), aquaporin 5 (*AQP5*), SAM pointed domain containing ETS transcription factor (*SPDEF*), anterior gradient protein 2 (*AGR2*), apolipoprotein B messenger RNA editing enzyme catalytic subunit 1 (*APOBEC1*), kallikrein-related peptidase 6 (*KLK6*), dopa decarboxylase (*DDC*), mucin 13 (*MUC13*), claudin 18 (*CLDN18*), annexin A10 (*ANXA10*), and tetraspanin 1 (*TSPAN1*) were found to be present in PAAD and had the largest fold change. A risk-score model, comprising 19 genes, was constructed for prognostic prediction. A high-risk score indicated a poor prognosis. *TINAG*, *DDC*, *SPDEF*, and *APOBEC1* proteins were increased in PAAD, while *TINAG* and *DDC* were correlated with the pathologic grade. Decreased *TINAG*, *APOBEC1*, transmembrane protein 94 (*TMEM94*), and kelch like family member 36 (*KLHL36*) expression inhibited PAAD cell proliferation, while decreased *SPDEF*, *TMEM94*, and *KLHL36* expression significantly inhibited PAAD cell migration.

Conclusions: The AP and CP co-related genes were significantly correlated with PAAD. TINAG, DDC, SPDEF, and APOBEC1 could serve as new PAAD predictors. The risk model developed in this study could be used to predict the prognosis of PAAD patients.

Keywords: Pancreatitis; pancreatic adenocarcinoma (PAAD); bioinformatics; diagnosis; prognosis

Submitted Jul 31, 2023. Accepted for publication Jan 11, 2024. Published online Mar 27, 2024.

doi: 10.21037/tcr-23-1365

View this article at: <https://dx.doi.org/10.21037/tcr-23-1365>

Introduction

The incidence of pancreatic cancer continues to increase both in China and abroad (1-3). Pancreatic adenocarcinoma (PAAD) is asymptomatic in its early stage, and the prognosis of PAAD patients is poor. Currently, there is a lack of specific diagnostic biomarkers for PAAD (4,5). Thus, advances need to be made in PAAD diagnosis or prognosis to improve PAAD patient survival.

It has been continuously demonstrated that long-term chronic pancreatitis (CP) is an important risk factor of PAAD. Patients with CP have a high risk of developing PAAD (6,7). Acinar cells, which secrete digestive enzymes, are thought to be very important in the inflammation of pancreatitis, causing ductal metaplasia, a precursor to pancreatic carcinogenesis. Inflammatory molecules also promote tumor growth through epithelial and mesenchymal secretion. These findings provide evidence that anti-inflammation agents could be a preventive and/or therapeutic agent for PAAD (8-11). Conversely, CP can develop from acute pancreatitis (AP). The evolution of AP-CP-PAAD is a prominent stage in PAAD onset and

development, and the co-expression of AP-CP genes may serve as potential new diagnostic and prognostic markers for early PAAD (12).

Bioinformatics is an emerging discipline that mainly includes biology, mathematics, and computer science, and is being rapidly developed by the Human Genome Project (13,14). The vast amount of biomedical data has helped to elucidate the relative biological knowledge and convey biological information more comprehensively and effectively. With the continuous accumulation of biological data and the launch of strategic planning for precision medicine, bioinformatics has become increasingly important and crucial to the current development of related fields (15).

In this article, based on the AP-CP-PAAD transformation and experimental validation studies using cancer-related databases, we investigated and validated new predictors for early PAAD diagnosis and prognosis. We present this article in accordance with the TRIPOD reporting checklist (available at <https://tcr.amegroups.com/article/view/10.21037/tcr-23-1365/rc>).

Methods

Data resource

Expression profile microarrays (GSE109227 and GSE41418) were obtained from the Gene Expression Omnibus (GEO) database (<https://www.ncbi.nlm.nih.gov/gds/>) for AP and CP mice, respectively, which are a genome-wide messenger RNA (mRNA) expression data (16). The GSE109227 data set contained six samples of AP tissue and five samples of normal pancreatic tissue. The GSE41418 data set contained six tissue samples of CP tissue and six samples of normal pancreatic tissue. Transcriptome sequencing (RNA-sequencing) data and matched clinical information data were obtained from The Cancer Genome Atlas (TCGA) database (<http://cancergenome.nih.gov>) for four normal controls and 150 PAAD cases with fragments

Highlight box

Key findings

- Acute pancreatitis (AP) and chronic pancreatitis (CP) co-related genes are significantly correlated with pancreatic adenocarcinoma (PAAD). TINAG, DDC, SPDEF, and APOBEC1 could serve as predictors of PAAD. The risk model developed in this study could be used to predict the prognosis of PAAD patients.

What is known, and what is new?

- Genes involved in AP/CP might be important for PAAD development.
- This report identified the genes involved in AP/CP/PAAD transformation.

What is the implication, and what should change now?

- AP could transform into PAAD in certain patients.

per kilobase per million mapped fragments (FPKM)-style data. Non-pancreatic ductal adenocarcinoma patients (27 cases) (17) and patients with no survival information (one case) were excluded from the survival analysis (18). A total of 182 cancer patient samples with complete survival prognosis data were screened from the International Cancer Genome Consortium (ICGC) database; all the available data from the database were used to maximize the power and generalizability of the results. The study was conducted in accordance with the Declaration of Helsinki (as revised in 2013).

Differential expression analysis and Venn analysis of shared common differentially expressed genes (co-DEGs)

An online differential analysis was performed of the GEO database data using GEO2R with the threshold set at $P < 0.05$ to identify the significantly differently expression genes in AP and CP. The shared co-DEGs in the GSE109227 and GSE41418 data sets were also analyzed by the online database VENNY 2.1 (<https://bioinfogp.cnb.csic.es/tools/venny/>). The list of genes to be analyzed was uploaded to the database to display the Venn diagram and the list of related shared genes (19).

Analysis of variance and one-way Cox regression analysis

Data on the survival time and survival status of PAAD patients were extracted; patients with a survival time of 0 days (one case) were removed. The survival time and status data were combined with the DEG data to form a matrix, and a differential analysis was first performed of the co-DEGs of the TCGA-PAAD data set. The threshold was set to $P < 0.05$. Using the “survival” package of R software, a one-way Cox regression analysis was performed, and a P value < 0.05 indicated that the DEG was related to the prognosis of PAAD patients. After the Venn analysis, the target genes were screened for association with both PAAD occurrence and prognosis. The “pheatmap” package was used to map a heat map of the target genes. A target gene forest map was then drawn using the survival package (20,21).

Prognostic risk-score model construction

Least absolute shrinkage and selection operator (LASSO) Cox regression analysis

The TCGA-PAAD cohort was analyzed by LASSO regression using L1 regularization statistics. Based on

the results of the one-way Cox regression analysis, the prognosis-related genes with P values < 0.05 were further analyzed using the LASSO regression algorithm of the “glmnet” R package, and the prognosis-related genes were further screened by a subsequent analysis based on the parameter Lambda values (22).

Model construction

Based on the regression coefficients obtained from the gene expression and multifactorial Cox regression analysis, a linear risk assessment model related to survival was constructed, and the coefficient value of each gene was obtained using the expression values of the genes in the model in each sample, the survival time, and the status data analysis results. The following formula was used to calculate the risk score for each pancreatic cancer patient in TCGA and the ICGC data sets, respectively: $\text{risk score} = \beta_1 \times \text{mRNA1EXP} + \beta_2 \times \text{mRNA2EXP} + \dots + \beta_n \times \text{mRNAnEXP}$. The risk model was constructed using 1000-times testing. A principal component analysis with t-distribution and randomized nearest neighbor embedding (t-SNE) was performed using the “Rtsne” R package to analyze the differentiation between the high-risk and low-risk groups of TCGA and the ICGC data sets, respectively, and the results were visualized by the “ggplot2” package of R software. Next, to assess whether the model could be used as a prognostic factor independent of other clinical features, the “survival” package of R software was used to perform univariate and multi-variate independent prognostic analyses, the results were visualized by drawing forest plots, and the “limma” R package was used for the risk difference analysis (23,24).

Clinical correlation analysis

The prognostic risk characteristics were analyzed by the “ggpubr” package of R software with patient age, gender, clinical grade or pathological stage, and the R package was used to plot each clinical characteristic. The box plots of clinical characteristics and patient risk scores were created using the R package.

Experiment-related materials and methods

Primary antibodies

Anti-tubulointerstitial nephritis antigen (TINAG) antibody was obtained from Proteintech (Wuhan, China). Anti-dopa decarboxylase (DDC), kelch like family member 36

(KLHL36), apolipoprotein B messenger RNA editing enzyme catalytic subunit 1 (APOBEC1), SAM pointed domain containing ETS transcription factor (SPDEF) antibodies were from Sangon Biotech (Shanghai) Co., Ltd.

Small-interfering RNA sequences

These sequences were synthesized by GenePharma (Shanghai, China) (Table 1).

Immunohistochemistry staining

The PAAD tissue microarrays were purchased from the Shanghai Core Ultra Biological Co., Ltd. (item no. HPanA020PG01), and the number of valid cancer tissue cases for the TINAG, DDC, SPDEF, APOBEC1, and KLHL36 detection chips was 20. The tissue samples were incubated with the anti-APOBEC1 (Shanghai Biotechnology Co., Ltd.) and anti-KLHL36 (Shanghai Biotechnology Co., Ltd.) polyclonal antibodies. Finally, the protein expression levels were scored under the microscope by multiple uninformed pathologists. The intensity and area of staining were categorized into the following four grades: 0 (negative), 1 (weakly positive), 2 (moderately positive), and 3 (strongly positive).

Cell proliferation assays

The cells under the indicated treatments were inoculated in 96-well plates (5,000 cells/well). The cells were plated, and incubated for 12, 24, 48, and 72 hours. The old medium was discarded and replaced with 100 μ L of new medium, or Cell Counting Kit-8 (CCK-8) reagent (10 μ L/well) was added and mixed well. The medium was then transferred to the cell incubator for 2 hours. The absorbance of the cells was measured at 450 nm with an enzyme marker.

Transwell migration assays

Transwell migration chambers were used. The cells were cultured in the upper chamber with complete medium in the lower chamber. The chambers were transferred to the incubator and removed after 24 hours. The cells were fixed and then underwent crystal violet staining. Cell migration in each well was observed under an inverted microscope, counted, and then statistically analyzed.

Pathway analysis of TINAG, DDC, SPDEF, and APOBEC1

The TINAG, DDC, SPDEF, and APOBEC1 genes were screened by TCGA-PAAD-RNA-sequencing genomic

screening through the online website LinkedOmics database (<https://www.linkedomics.org/login.php>) to obtain the relevant co-expression gene clusters. The relevant co-expression gene clusters were then subjected to a Gene Set Enrichment Analysis-Kyoto Encyclopedia of Genes and Genomes (KEGG) enrichment analysis via the online WebGestalt database (<https://www.webgestalt.org/>), and the pathway atlas was obtained.

Statistical analysis

All the bioinformatics analyses were performed in R software (version 3.6.1). The remaining statistical analyses were performed using SPSS software (version 25.0) and GraphPad Prism software (version 9.0). The following P values were considered statistically significant: *, $P < 0.05$; **, $P < 0.01$; ***, $P < 0.001$; ****, $P < 0.0001$.

Results

Co-expression analysis of DEGs in AP and CP

The GSE109227 data set, which contained six mouse AP tissue samples and five matched normal control tissue samples, was selected first. The DEGs were screened using GEO2R and are presented in a volcano plot (Figure 1A). A total of 12,007 AP-DEGs were identified in the AP data set. Similarly, the GSE41418 data set, which contained six mouse CP tissue samples and six matched normal control tissue samples, was next selected to screen the DEGs in CP (Figure 1B). A total of 7,479 CP-DEGs were identified in the CP data set. Next, to identify the DEGs common to AP and CP, we analyzed the intersecting genes between the AP-DEGs and CP-DEGs (i.e., the co-DEGs) through the online database VENNY 2.1. In total, 4,506 co-DEGs were identified (Figure 1C). Additionally, 3,453 co-DEGs were identified in TCGA data set.

Differential analysis of the co-DEGs in TCGA-PAAD

Among the 3,453 co-DEGs, 508 co-DEGs were found to be differentially expressed in PAAD, while 457 co-DEGs were correlated with PAAD prognosis. Specifically, trefoil factor 2 (TFF2), TINAG, trefoil factor 1 (TFF1), aquaporin 5 (AQP5), SPDEF, anterior gradient protein 2 (AGR2), APOBEC1, kallikrein-related peptidase 6 (KLK6), DDC, mucin 13 (MUC13), claudin 18 (CLDN18), annexin A10 (ANXA10), and tetraspanin 1 (TSPAN1) presented with

Table 1 Small RNA interfering sequences

Gene name	Company	Sequence (5'-3')
TINAG-Homo-115	GenePharma	Positive: GGACCGGAUUAAGAUCUUTT Trans: AAGAUCUUUAUCCGGUCCTT
TINAG-Homo-540	GenePharma	Positive: GGACAGCAAUGGAAAUGUUTT Trans: AACAUUUCCAUUGCUGUCCTT
TINAG-Homo-795	GenePharma	Positive: GGAUGGACUCAUGGCCAUTT Trans: AUGGGCCAUGAGUCCAUCCTT
DDC-Homo-311	GenePharma	Positive: GGACAUCAUCAACGACGUUTT Trans: AACGUCGUUGAUGAUGUCCTT
DDC-Homo-720	GenePharma	Positive: GCACACUCCUCAGUGGAAATT Trans: UUUCCACUGAGGAGUGUGCTT
DDC-Homo-895	GenePharma	Positive: GCUCCUUUGACAAUCUCUUTT Trans: AAGAGAUUGUCAAGGAGCTT
KLHL36-Homo-191	GenePharma	Positive: GCCAUACAAGAUCAAGCAATT Trans: UUCGCUGAUCUUGUAUGGCTT
KLHL36-Homo-358	GenePharma	Positive: GCGACUACUUAACUCCAUTT Trans: AUGGAGUUGAAGUAGUCGCTT
KLHL36-Homo-1235	GenePharma	Positive: GGAUGCGGCCUCCAUCUUTT Trans: AAGAUUGGAGGCCGCAUCCTT
APOBEC1-Homo-99	GenePharma	Positive: GGAGUUUGACGUCUUCUAUTT Trans: AUAGAAGACGUCAAACUCCTT
APOBEC1-Homo-142	GenePharma	Positive: GCCUGUCUGUCUACGAAATT Trans: UUCGUGAGAGCAGACAGGCTT
APOBEC1-Homo-318	GenePharma	Positive: GGAAUGCUCAGGCUAUUTT Trans: AAUAGCCUGGGAGCAUUCCTT
SPDEF-Homo-839	GenePharma	Positive: GCCUGCAAGCUGCUC AACATT Trans: UGUUGAGCAGCUUGCAGGCTT
SPDEF-Homo-1227	GenePharma	Positive: GCCGCUUCAUAGUGGCUTT Trans: AGCCACCUAAUGAAGCGGCTT
TMEM94-Homo-1337	GenePharma	Positive: GCUGUCUCCUCUCAGGAAATT Trans: UUUCCUGAGAGGAGACAGCTT
TMEM94-Homo-1506	GenePharma	Positive: GCCCAGAGACUGUACUGUUTT Trans: AACAGUACAGUCUCUGGGCTT
TMEM94-Homo-1980	GenePharma	Positive: GCCUCAUUGUGCUGCUGAATT Trans: UUCAGCAGCACAUUGAGGCTT

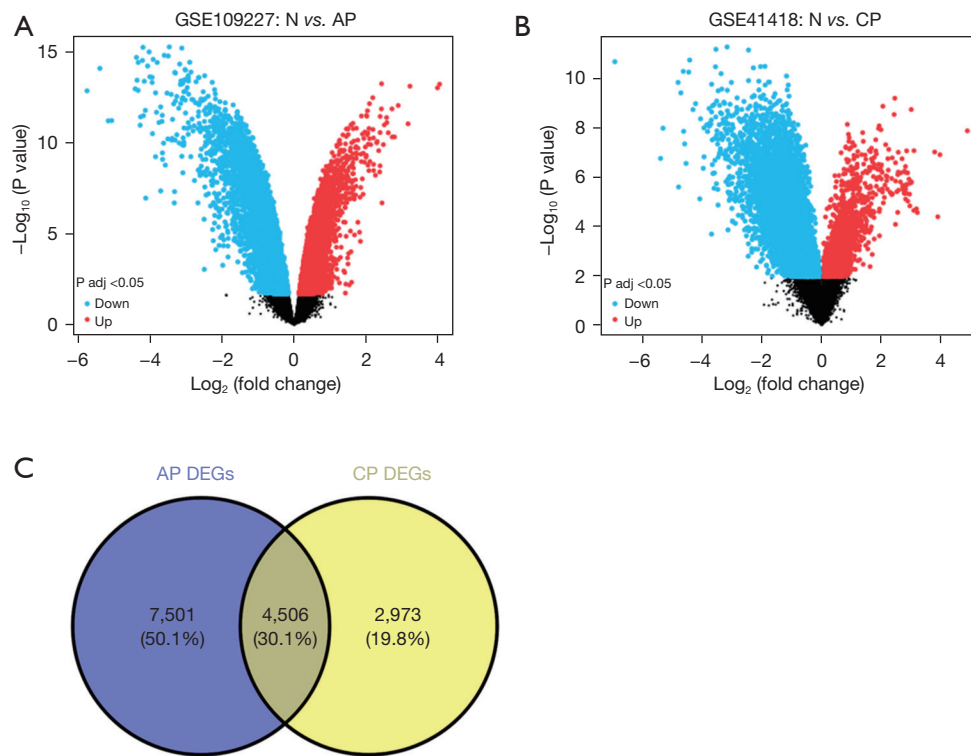


Figure 1 DEG screening of AP and CP. (A) Volcano plot of GSE109227 for AP. (B) Volcano plot of GSE41418 for CP. (C) Venn diagram of co-DEGs in AP and CP. Blue dots: down-regulated genes; red dots: up-regulated genes; black dots: genes with no changes. N, normal; AP, acute pancreatitis; CP, chronic pancreatitis; P adj, adjusted P value; DEGs, differentially expressed genes.

the largest fold expression changes in PAAD (i.e., a log fold change >3) (Table 2). The two groups of genes were then subjected to Venn analysis. We found that 116 genes (which we refer to as target gene clusters) were closely associated with both PAAD development and prognosis (Figure 2A). The expression of the target gene clusters in PAAD is shown in a heat map (Figure 2B). A forest plot of these genes in PAAD is also presented. In total, 28 up-regulated genes and 88 down-regulated genes were found (Figure 2C).

Risk-score model construction

PAAD patient data downloaded from TCGA or the ICGC databases were used as training and validation sets. A LASSO regression analysis was conducted on the above 116 target gene groups, and the following 19 key prognosis-related genes were identified: enoyl-CoA hydratase and 3-hydroxyacyl CoA dehydrogenase (*EHHADH*), MET Proto-Oncogene, Receptor Tyrosine Kinase (*MET*), DNA methyltransferase 3 alpha (*DNMT3A*), Rho GTPase activating protein 17 (*ARHGAP17*), tubulin tyrosine ligase

(*TTL*), EGFR pathway substrate 8, signaling adaptor (*EPS8*), BCL11 transcription factor A (*BCL11A*), *KLHL36*, differentially expressed in FDCP 8 homolog (*DEF8*), RELB proto-oncogene, NF- κ B subunit (*RELB*), crystallin alpha B (*CRYAB*), transmembrane protein 94 (*TMEM94*), cell division cycle 20 (*CDC20*), solute carrier family 16 member 14 (*SLC16A14*), cyclin B2 (*CCNB2*), nectin cell adhesion molecule 3 (*NECTIN3*), anillin, actin binding protein (*ANLN*), amyloid beta precursor protein binding family A member 1 (*APBA1*), and DNA topoisomerase II alpha (*TOP2A*) (Figure 3A, 3B and Table 3). The following risk-score equation based on the expression of the 19 key genes was formulated: $0.08945 \times EHHADH + 0.24165 \times MET + (-0.12536) \times DNMT3A + (-0.54232) \times ARHGAP17 + (-0.1063) \times TTL + 0.244083 \times EPS8 + (-0.03683) \times BCL11A + (-0.46656) \times KLHL36 + (-0.00994) \times DEF8 + (-0.29732) \times RELB + (-0.0521) \times CRYAB + (-0.4635) \times TMEM94 + 0.118142 \times CDC20 + (-0.03301) \times SLC16A14 + 0.170268 \times CCNB2 + 0.001 \times NECTIN3 + 0.075642 \times ANLN + (-0.62613) \times APBA1 + 0.096801 \times TOP2A$.

Risk scores were calculated for each PAAD patient in

Table 2 Genes with the largest fold expression changes in PAAD cases compared with controls among co-DEGs

Gene	Control	PAAD	logFC	P value
<i>TFF2</i>	6.83664	267.8866	5.292191	0.002974
<i>TINAG</i>	0.033313	1.003763	4.913173	0.005472
<i>TFF1</i>	40.79442	802.0375	4.297226	0.007221
<i>AQP5</i>	2.230661	41.41324	4.214549	0.002468
<i>SPDEF</i>	1.084305	18.34634	4.08065	0.001386
<i>AGR2</i>	13.91381	211.2185	3.924146	0.001386
<i>APOBEC1</i>	0.426995	6.257341	3.873257	0.008128
<i>KLK6</i>	2.854156	40.6557	3.832321	0.009135
<i>DDC</i>	0.24065	2.951894	3.616632	0.007471
<i>MUC13</i>	5.292654	60.24678	3.508821	0.002562
<i>CLDN18</i>	11.69363	126.2321	3.432284	0.021434
<i>ANXA10</i>	7.037711	67.75781	3.267209	0.016284
<i>TSPAN1</i>	17.2421	142.9409	3.051412	0.002204

PAAD, pancreatic adenocarcinoma; co-DEGs, common differentially expressed genes; FC, fold change.

both TCGA and the ICGC data sets, and the patients were divided into high- and low-risk groups. The study found a significant difference in overall survival between the high- and low-risk groups for TCGA-PAAD (Figure 3A-3C). The high-risk group had a worse prognosis and shorter survival time than the low-risk group. The univariate and multifactor independent prognostic analyses showed that the N stage and risk-score value were independent risk factors for PAAD prognostic (Figure 3D). A receiver operating characteristic (ROC) curves analysis was conducted to further investigate the diagnostic efficiency of the risk-score model in TCGA data set. The areas under the curve (AUCs) for 1-, 2- and 3-year survival were 0.871, 0.8, and 0.782, respectively, indicating that the model was good at predicting PAAD patient survival (Figure 3E).

The risk score was validated in the ICGC-PAAD data set. Consistent with TCGA results, the high-risk group had a worse prognosis and shorter survival time than the low-risk group ($P < 0.05$, Figure 3F). A ROC curve analysis was conducted to further investigate the diagnostic efficiency of the risk-score model in the ICGC data set. The AUCs for 1-, 2- and 3-year survival were 0.624, 0.696, and 0.613, respectively (Figure 3G). Taken together, the results indicate that the risk score can be used to predict PAAD patient survival.

Immunohistochemical validation

The expression of the genes related to PAAD occurrence, including *TINAG*, *DDC*, *SPDEF*, and *APOBEC1*, were tested in clinic samples. The *TINAG*, *DDC*, *SPDEF*, and *APOBEC1* proteins increased as the tumor pathological grade increased. However, only *TINAG* and *DDC* were significantly differentially expressed in grades I and II ($P < 0.05$) (Figures 4, 5). In addition, 19 key genes in the prognosis risk model were also tested in the clinic samples. As observed in the risk model, *KLHL36* was negatively associated with a poor prognosis; however, our results showed that *KLHL36* protein expression was significantly more increased in grade II than grade I patients ($P < 0.05$) (Figures 4, 5).

Effects of *SPDEF*, *TINAG*, *DDC*, *APOBEC1*, *TMEM94*, and *KLHL36* on PAAD cell growth

SPDEF, *TINAG*, *DDC*, *APOBEC1*, *TMEM94*, and *KLHL36* were knocked down, and the proliferation of PAAD cells was investigated by CCK-8 cell assays (Figure 6). The results showed that the proliferation of PAAD cells was significantly inhibited following the knock down of *TINAG*, *APOBEC1*, *TMEM94*, and *KLHL36* (at 48 and 72 hours) (Figure 6B, 6D-6F). However, the knock down of *SPDEF*

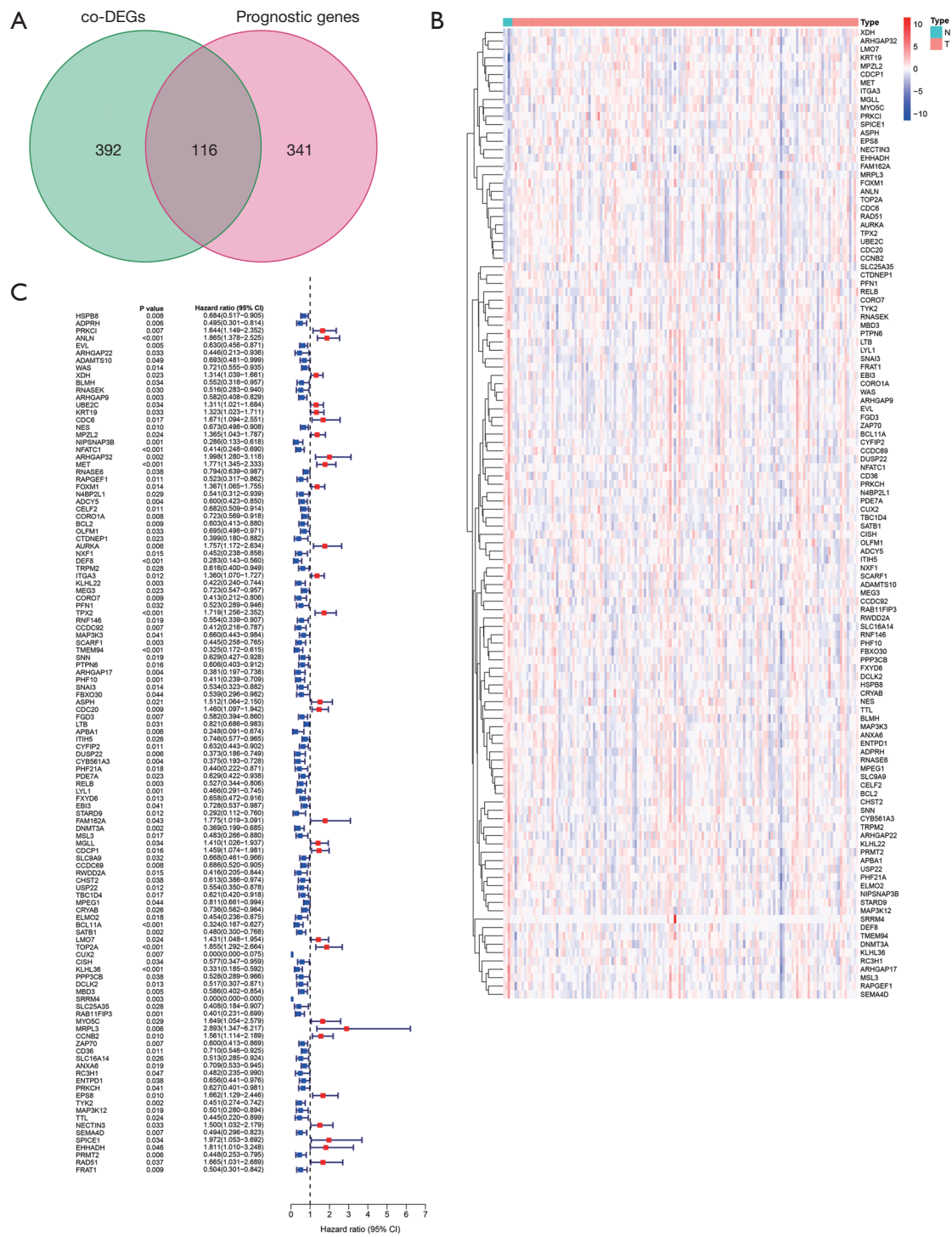


Figure 2 TCGA-PAAD prognostic DEG screening. (A) Venn diagram of prognostic DEGs in pancreatic cancer based on the co-DEGs. (B) Heat map of the expression of the target gene groups in PAAD. (C) Forest plot of the target gene groups in PAAD. co-DEGs, common differentially expressed genes; N, normal; T, tumor; CI, confidence interval; TCGA, The Cancer Genome Atlas; PAAD, pancreatic adenocarcinoma.

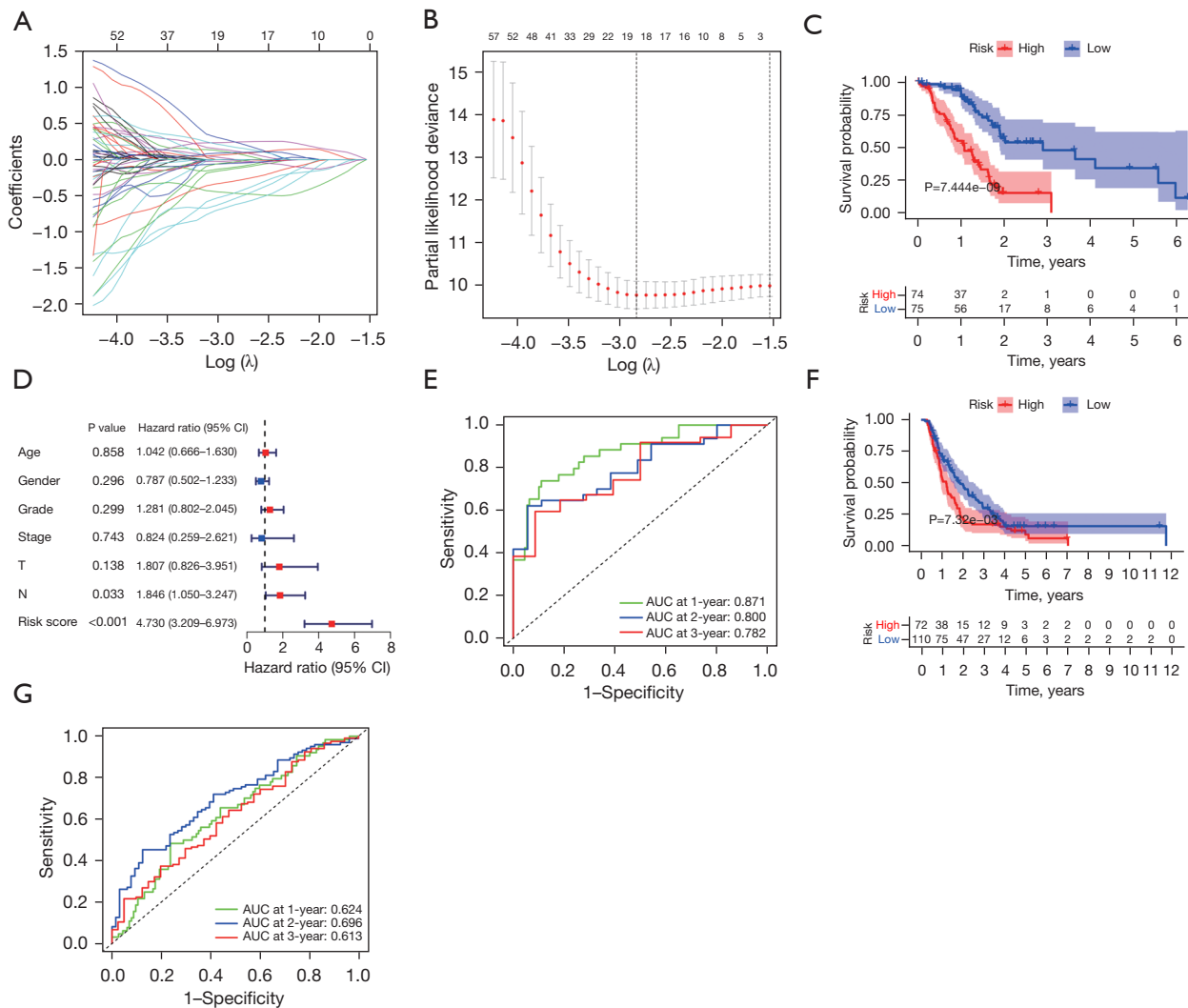


Figure 3 Construction of risk-score model by LASSO Cox regression analysis. (A) LASSO regression was used to determine the optimal λ value. (B) LASSO regression curve. (C) OS survival curves between TCGA high- and low-risk groups. (D) TCGA univariate independent prognostic analysis. (E) Risk score predicts TCGA 1-, 2-, and 3-year survival ROC curves. (F) OS survival curve between ICGC high- and low-risk groups. (G) Risk score predicts ICGC 1-, 2-, and 3-year survival ROC curves. CI, confidence interval; AUC, area under curve; LASSO, least absolute shrinkage and selection operator; OS, overall survival; TCGA, The Cancer Genome Atlas; ROC, receiver operating characteristic; ICGC, International Cancer Genome Consortium.

and *DDC* did not affect the proliferation of PAAD cells (Figure 6A,6C). These results suggest that *TINAG*, *APOBEC1*, *TMEM94*, and *KLHL36* inhibit the proliferation of PAAD cells.

Effects of *SPDEF*, *TINAG*, *DDC*, *APOBEC1*, *TMEM94*, and *KLHL36* on PAAD cell migration

To verify the effect of the above genes on PAAD cell migration, we performed transwell assays. The results

Table 3 Risk-score formula

Gene symbol	Description	Coefficient
<i>EHHADH</i>	Enoyl-CoA hydratase and 3-hydroxyacyl CoA dehydrogenase	0.08945
<i>MET</i>	MET Proto-Oncogene, Receptor Tyrosine Kinase	0.24165
<i>DNMT3A</i>	DNA methyltransferase 3 alpha	-0.12536
<i>ARHGAP17</i>	Rho GTPase activating protein 17	-0.54232
<i>TTL</i>	Tubulin tyrosine ligase	-0.1063
<i>EPS8</i>	EGFR pathway substrate 8, signaling adaptor	0.244083
<i>BCL11A</i>	BCL11 transcription factor A	-0.03683
<i>KLHL36</i>	Kelch like family member 36	-0.46656
<i>DEF8</i>	Differentially expressed in FDCP 8 homolog	-0.00994
<i>RELB</i>	RELB proto-oncogene, NF-kB subunit	-0.29732
<i>CRYAB</i>	Crystallin alpha B	-0.0521
<i>TMEM94</i>	Transmembrane protein 94	-0.4635
<i>CDC20</i>	Cell division cycle 20	0.118142
<i>SLC16A14</i>	Solute carrier family 16 member 14	-0.03301
<i>CCNB2</i>	Cyclin B2	0.170268
<i>NECTIN3</i>	Nectin cell adhesion molecule 3	0.001
<i>ANLN</i>	Anillin, actin binding protein	0.075642
<i>APBA1</i>	Amyloid beta precursor protein binding family A member 1	-0.62613
<i>TOP2A</i>	DNA topoisomerase II alpha	0.096801

showed that the down-regulation of *SPDEF*, *TMEM94*, and *KLHL36* significantly inhibited PAAD cell migration (Figure 7). However, the down-regulation of *TINAG*, *DDC*, and *APOBEC1* did not affect the migratory ability of PAAD cells.

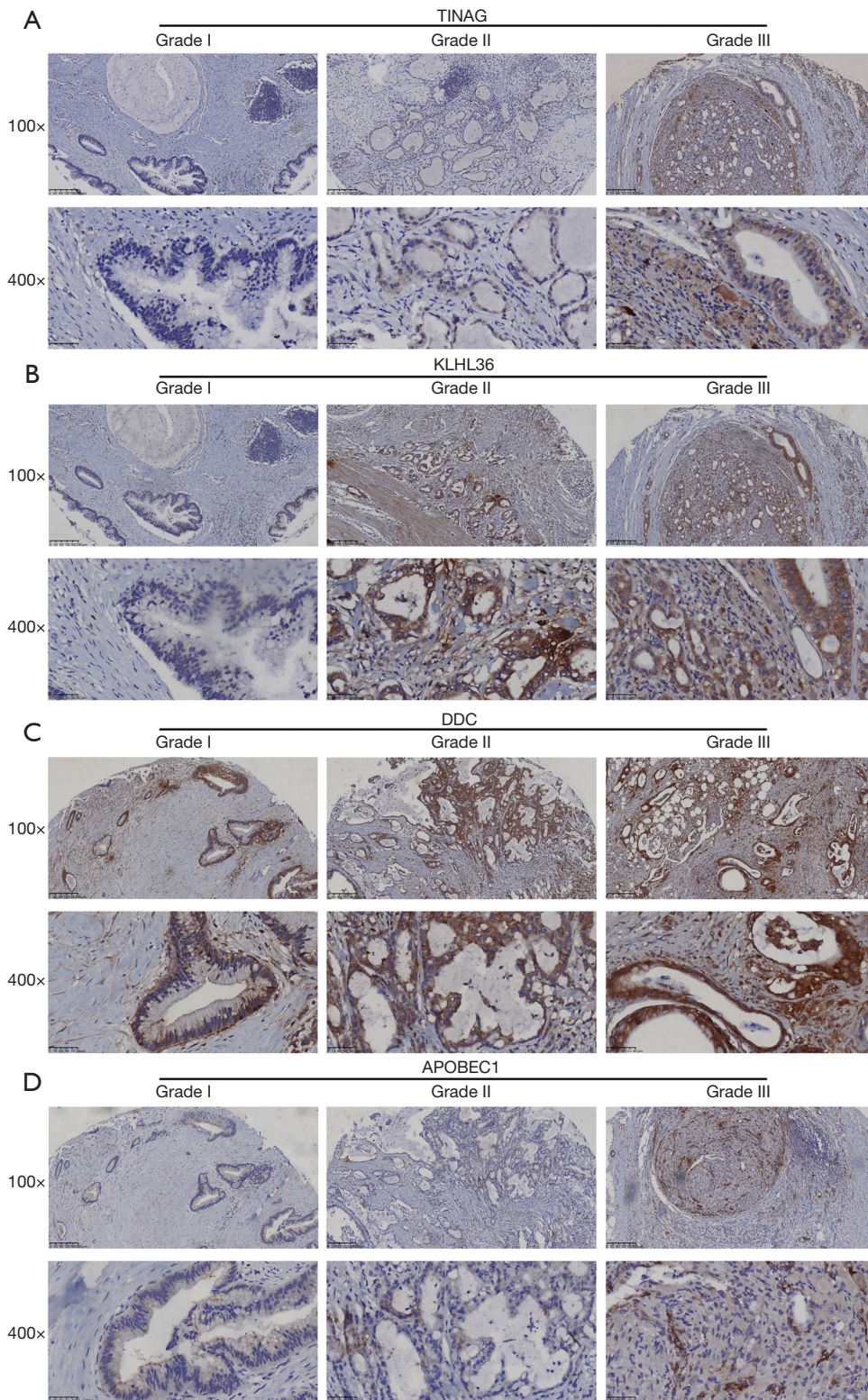
Pathway analysis for *TINAG*, *DDC*, *SPDEF*, and *APOBEC1*

Based on the above results, *TINAG*, *DDC*, *SPDEF*, and *APOBEC1* appear to be very important in PAAD occurrence. Thus, we analyzed the pathways in which these genes were involved. The results showed that in pancreatic cancer, the *TINAG*, *DDC*, *SPDEF*, and *APOBEC1* genes may be involved in the following pathways: neuroactive ligand-receptor interactions, cytokine-receptor interactions, natural killer cell-mediated cytotoxicity, cancer pathways, cancer proteoglycans, the extracellular matrix (ECM)-receptor interaction, the tumor necrosis factor (TNF)

signaling pathway, the repressor activator protein 1 (RAP1) signaling pathway, the Hippo signaling pathway, focal adhesion, tight junction, mannose type O-glycan biosynthesis, etc. (Figure 8). Meanwhile, we also found that some pathways were related to AP/CP, including apoptosis, the protein 53 (p53) signaling pathway, the phosphatidylinositol 3-kinase (PI3K)-Akt signaling pathway, the cell cycle, the cytokine-cytokine receptor interaction, glutathione metabolism, the regulation of actin cytoskeleton, leukocyte transendothelial migration, the metabolism of xenobiotics by cytochrome P450, necroptosis, linoleic acid metabolism, glycerophospholipid metabolism peroxisome, porphyrin and chlorophyll metabolism, and proteasome (Figure 8).

Discussion

In this study, we used data sets from mice with AP or CP from the GEO database. AP and CP could be clearly



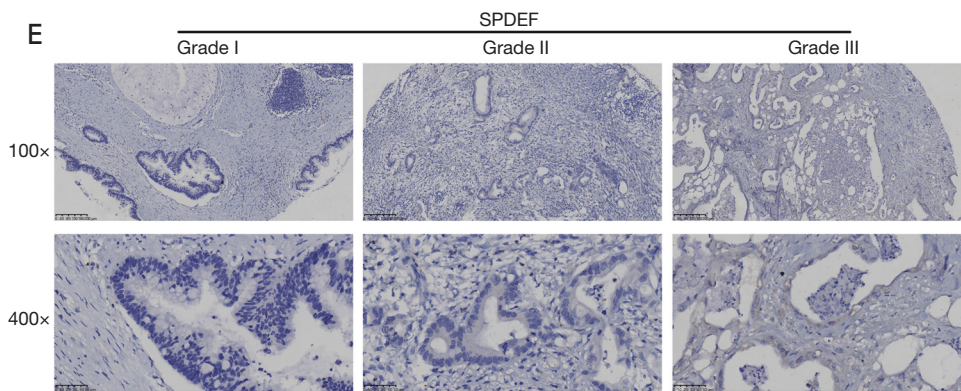


Figure 4 IHC results of indicated proteins in clinic samples with different pathological grades. TINAG, tubulointerstitial nephritis antigen; KLHL36, kelch like family member 36; DDC, dopa decarboxylase; APOBEC1, apolipoprotein B messenger RNA editing enzyme catalytic subunit 1; SPDEF, SAM pointed domain containing ETS transcription factor; IHC, immunohistochemistry.

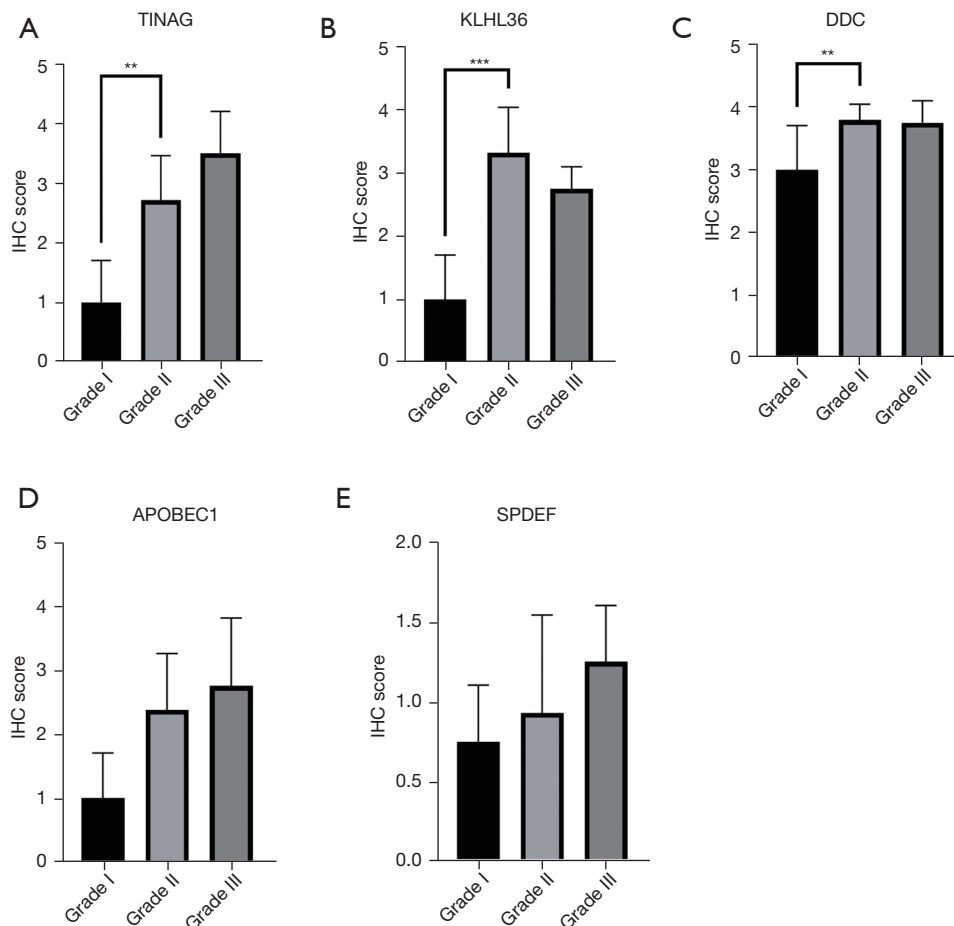


Figure 5 The relationship between the indicated proteins and pathological grade. **, $P < 0.01$; ***, $P < 0.001$. TINAG, tubulointerstitial nephritis antigen; KLHL36, kelch like family member 36; DDC, dopa decarboxylase; APOBEC1, apolipoprotein B messenger RNA editing enzyme catalytic subunit 1; SPDEF, SAM pointed domain containing ETS transcription factor; IHC, immunohistochemistry.

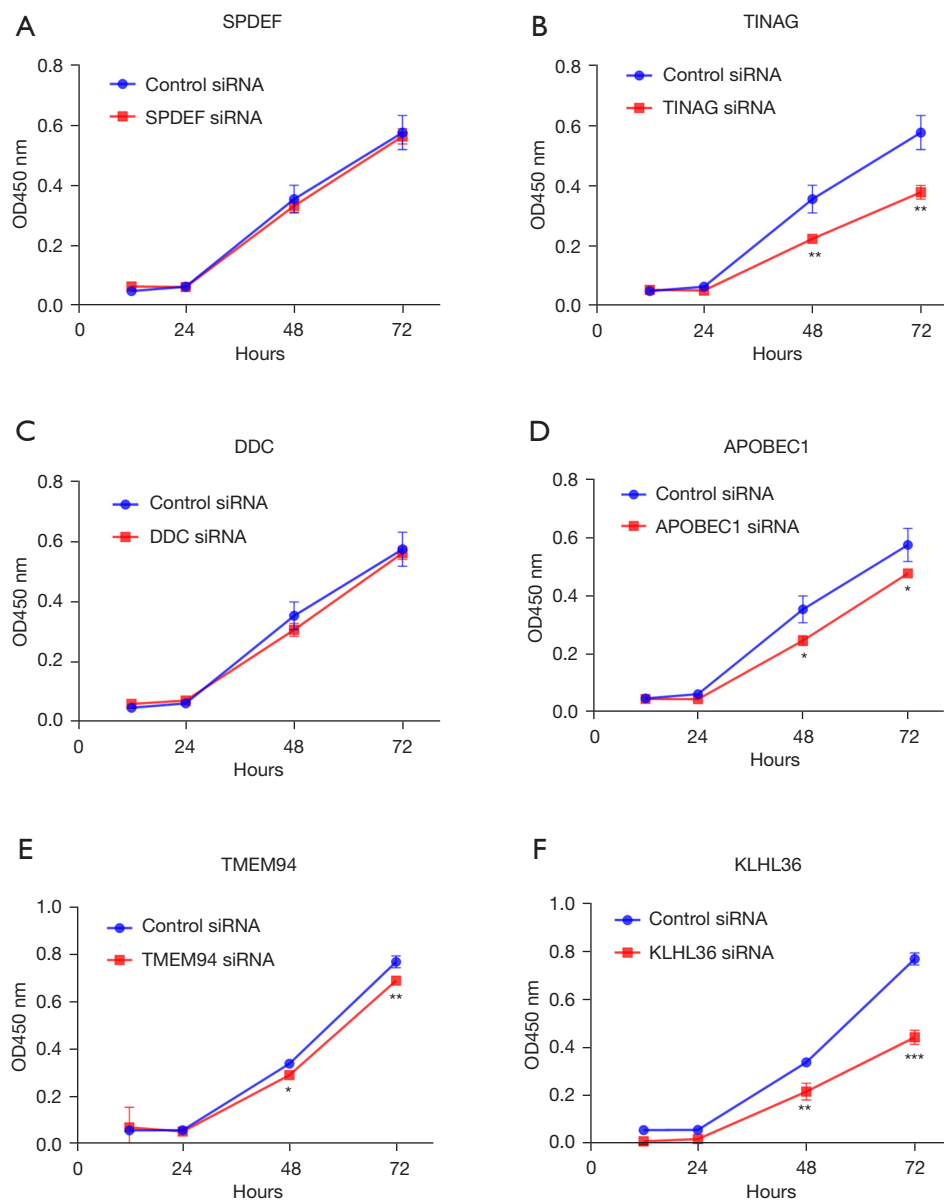


Figure 6 Effects of the down-regulation of each indicated genes on the proliferation of PAAD cells. *, $P < 0.05$; **, $P < 0.01$; ***, $P < 0.001$. OD, optical density; *SPDEF*, SAM pointed domain containing ETS transcription factor; *TINAG*, tubulointerstitial nephritis antigen; *DDC*, dopa decarboxylase; *APOBEC1*, apolipoprotein B messenger RNA editing enzyme catalytic subunit 1; *TMEM94*, transmembrane protein 94; *KLHL36*, kelch like family member 36; PAAD, pancreatic adenocarcinoma.

determined in mouse that were not so easy in the clinic (25). However, the use of mouse models also had some disadvantages. Notably, there are differences in gene expression between humans and mice in both protein-coding and non-coding genes (26).

In this study, we found that *TFF2*, *TINAG*, *TFF1*, *AQP5*, *SPDEF*, *AGR2*, *APOBEC1*, *KLK6*, *DDC*, *MUC13*,

CLDN18, *ANXA10*, and *TSPAN1* may be potential early diagnostic markers for PAAD. Among them, *TFF2*, *TFF1*, *AGR2*, *AQP5*, *KLK6*, *MUC13*, *CLDN18*, *ANXA10*, and *TSPAN1* have been found to be expressed in PAAD (27-34). These genes have been shown to affect the occurrence, development, and metastasis of PAAD through multiple pathways and regulatory networks (28). Consistent with

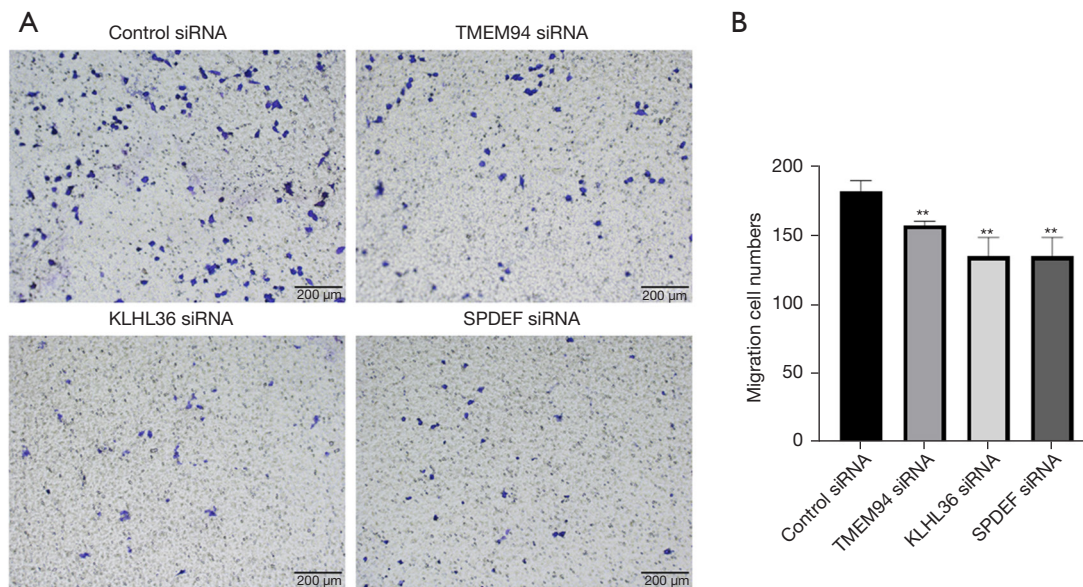


Figure 7 Effects of the down-regulation of each indicated genes on the migration of PAAD cells. Cells treated as indicated were cultured in transwell migration chambers. Cell migration in each well was stained with crystal violet and observed under an inverted microscope, counted, and then statistically analyzed. **, $P < 0.01$. *TMEM94*, transmembrane protein 94; *KLHL36*, kelch like family member 36; *SPDEF*, SAM pointed domain containing ETS transcription factor; PAAD, pancreatic adenocarcinoma.

previous research (27–34), we found that *TFF2*, *TFF1*, *AGR2*, *AQP5*, *KLK6*, *MUC13*, *CLDN18*, *ANXA10*, and *TSPAN1* mRNAs were highly expressed in PAAD. Thus, a significant portion of our screened target genes were found to be associated with PAAD, which provides supporting evidence of the feasibility of our analytical approach. Notably, the AP-CP-PAAD mechanism plays a key role in the development of PAAD.

The associations between *TINAG*, *DDC*, *SPDEF*, and *APOBEC1* and PAAD had not previously been examined. The bioinformatics analysis also found that the fold changes of the genes in PAAD were larger than those in AP or CP. Together, the immunohistochemistry and cellular assay results suggest that *TINAG* is the potential new early diagnostic marker for PAAD.

According to the prognostic risk-score model consisting of 19 genes, *MET* and *ANLN* were positively associated with a poor prognosis in PAAD, while *DNMT3A*, *KLHL36*, *DEF8*, and *TMEM94* were negatively associated with a poor prognosis in PAAD. The hepatocyte growth factor (HGF)/*MET* signaling pathway promotes the motility, histomorphogenesis and mesenchymal-epithelial transition of epithelial cells in the body (35), and also plays a role in the development and progression of many mesenchymal-derived tumors (36). *DNMT3A* promotes proliferation by

activating the signal transducer and activator of transcription 3 (*STAT3*) signaling pathway and inhibiting apoptosis in PAAD (37). Bioinformatics analysis results have identified *DEF8* and *MET* in a risk scoring system for predicting the prognosis of patients with resectable PAAD (38). The experiments were not validated; however, the reliability of this model was confirmed by previous finding. *ANLN* was included in another risk-score model for overall survival prediction (39). All these findings support the conclusion reached by this study.

A study screening of AAD diagnostic markers from CP-related genes identified *CCNB2*, cell division cycle 6 (*CDC6*), cyclin-dependent kinase 1 (*CDK1*), cell division cycle 28 (*CDC28*), and cyclin-dependent kinase regulatory subunit 2 (*CKS2*) as key genes involved in the development of CP and PAAD (40). Another study conducted a microarray (Affymetrix) analysis and identified four DEGs in PAAD and CP; that is, 14-3-3sigma, S100 calcium binding protein P (*S100P*), S100 calcium binding protein A6 (*S100A6*), and integrin beta4 (*ITGB4*) (41). Unlike previous studies, we innovatively searched for new key genes associated with PAAD initiation, progression and metastasis from the AP-CP-PAAD perspective, thus potentially identifying key genes that play a role in the early stage of pancreatic cancer.

In the process of our research, we found a relationship



Figure 8 Pathways analysis for *DDC* (A), *APOBEC1* (B), *SPDEF* (C), and *TINAG* (D). FDR, false discovery rate; *DDC*, dopa decarboxylase; *APOBEC1*, apolipoprotein B messenger RNA editing enzyme catalytic subunit 1; *SPDEF*, SAM pointed domain containing ETS transcription factor; *TINAG*, tubulointerstitial nephritis antigen.

between the genes related to AP, CP, and PAAD. In this study, we found that *TINAG*, *DDC*, *SPDEF*, and *APOBEC1* showed large fold changes in tumors and can serve as new diagnostic markers for PAAD. A risk-score risk model can be used as a new tool for PAAD prognosis prediction. However, more trials and clinical studies need to be conducted.

Conclusions

TINAG, *DDC*, *SPDEF*, and *APOBEC1* may serve as new early diagnostic markers for PAAD. The models constructed, which include *EHHADH*, *MET*, *DNMT3A*, *ARHGAP17*, *TTL*, *EPS8*, *BCL11A*, *KLHL36*, *DEF8*, *RELB*, *CRYAB*, *TMEM94*, *CDC20*, *SLC16A14*, *CCNB2*, *NECTIN3*, *ANLN*, *APBA1*, and *TOP2A*, may serve as potential diagnostic criteria for PAAD and indicators for the prognostic assessment of PAAD.

Acknowledgments

Funding: The present study was supported in part by the Natural Science Foundation of Guangxi Province (Nos. 2020GXNSFAA297254 and 2022GXNSFAA035509), the National Natural Science Foundation of China (No. 81960127), the Guangxi Medical and Health Key Discipline Construction Project, and the Recruitment Program for the Affiliated Hospital of Guilin Medical University, and by a grant from the Guangxi Key Laboratory of Molecular Medicine in Liver Injury and Repair. The funders had no role in the design of the study, in the collection, analyses, or interpretation of data, in the writing of the manuscript, or in the decision to publish the results.

Footnote

Reporting Checklist: The authors have completed the TRIPOD reporting checklist. Available at <https://tcr.amegroups.com/article/view/10.21037/tcr-23-1365/rc>

Data Sharing Statement: Available at <https://tcr.amegroups.com/article/view/10.21037/tcr-23-1365/dss>

Peer Review File: Available at <https://tcr.amegroups.com/article/view/10.21037/tcr-23-1365/prf>

Conflicts of Interest: All authors have completed the ICMJE uniform disclosure form (available at <https://tcr.amegroups.com/article/view/10.21037/tcr-23-1365/coif>).

The authors have no conflicts of interest to declare.

Ethical Statement: The authors are accountable for all aspects of the work in ensuring that questions related to the accuracy or integrity of any part of the work are appropriately investigated and resolved. The study was conducted in accordance with the Declaration of Helsinki (as revised in 2013).

Open Access Statement: This is an Open Access article distributed in accordance with the Creative Commons Attribution-NonCommercial-NoDerivs 4.0 International License (CC BY-NC-ND 4.0), which permits the non-commercial replication and distribution of the article with the strict proviso that no changes or edits are made and the original work is properly cited (including links to both the formal publication through the relevant DOI and the license). See: <https://creativecommons.org/licenses/by-nc-nd/4.0/>.

References

- Jia X, Du P, Wu K, et al. Pancreatic Cancer Mortality in China: Characteristics and Prediction. *Pancreas* 2018;47:233-7.
- Miller KD, Nogueira L, Devasia T, et al. Cancer treatment and survivorship statistics, 2022. *CA Cancer J Clin* 2022;72:409-36.
- Kolbeinsson HM, Chandana S, Wright GP, et al. Pancreatic Cancer: A Review of Current Treatment and Novel Therapies. *J Invest Surg* 2023;36:2129884.
- National Health Commission Of The People's Republic Of China. National guidelines for diagnosis and treatment of pancreatic cancer 2022 in China (English version). *Chin J Cancer Res* 2022;34:238-55.
- Stoffel EM, Brand RE, Goggins M. Pancreatic Cancer: Changing Epidemiology and New Approaches to Risk Assessment, Early Detection, and Prevention. *Gastroenterology* 2023;164:752-65.
- Gandhi S, de la Fuente J, Murad MH, et al. Chronic Pancreatitis Is a Risk Factor for Pancreatic Cancer, and Incidence Increases With Duration of Disease: A Systematic Review and Meta-analysis. *Clin Transl Gastroenterol* 2022;13:e00463.
- Munigala S, Subramaniam DS, Subramaniam DP, et al. Incidence and Risk of Pancreatic Cancer in Patients with a New Diagnosis of Chronic Pancreatitis. *Dig Dis Sci* 2022;67:708-15.

8. Pinho AV, Chantrill L, Rooman I. Chronic pancreatitis: a path to pancreatic cancer. *Cancer Lett* 2014;345:203-9.
9. Hausmann S, Kong B, Michalski C, et al. The role of inflammation in pancreatic cancer. *Adv Exp Med Biol* 2014;816:129-51.
10. Padoan A, Plebani M, Basso D. Inflammation and Pancreatic Cancer: Focus on Metabolism, Cytokines, and Immunity. *Int J Mol Sci* 2019;20:676.
11. Wang L, Xie D, Wei D. Pancreatic Acinar-to-Ductal Metaplasia and Pancreatic Cancer. *Methods Mol Biol* 2019;1882:299-308.
12. Keihanian T, Barkin JA, Souto EO. Early Detection of Pancreatic Cancer: Risk Factors and the Current State of Screening Modalities. *Gastroenterol Hepatol (N Y)* 2021;17:254-62.
13. Collins FS, Patrinos A, Jordan E, et al. New goals for the U.S. Human Genome Project: 1998-2003. *Science* 1998;282:682-9.
14. Martin-Sanchez F, Iakovidis I, Nørager S, et al. Synergy between medical informatics and bioinformatics: facilitating genomic medicine for future health care. *J Biomed Inform* 2004;37:30-42.
15. Branco I, Choupina A. Bioinformatics: new tools and applications in life science and personalized medicine. *Appl Microbiol Biotechnol* 2021;105:937-51.
16. Barrett T, Edgar R. Gene expression omnibus: microarray data storage, submission, retrieval, and analysis. *Methods Enzymol* 2006;411:352-69.
17. Nicolle R, Raffenne J, Paradis V, et al. Prognostic Biomarkers in Pancreatic Cancer: Avoiding Errata When Using the TCGA Dataset. *Cancers (Basel)* 2019;11:126.
18. Tomczak K, Czerwińska P, Wiznerowicz M. The Cancer Genome Atlas (TCGA): an immeasurable source of knowledge. *Contemp Oncol (Pozn)* 2015;19:A68-77.
19. Sun L, Dong S, Ge Y, et al. DiVenn: An Interactive and Integrated Web-Based Visualization Tool for Comparing Gene Lists. *Front Genet* 2019;10:421.
20. Benítez-Parejo N, Rodríguez del Águila MM, Pérez-Vicente S. Survival analysis and Cox regression. *Allergol Immunopathol (Madr)* 2011;39:362-73.
21. Koletsi D, Pandis N. Survival analysis, part 3: Cox regression. *Am J Orthod Dentofacial Orthop* 2017;152:722-3.
22. D'Angelo GM, Rao D, Gu CC. Combining least absolute shrinkage and selection operator (LASSO) and principal-components analysis for detection of gene-gene interactions in genome-wide association studies. *BMC Proc* 2009;3 Suppl 7:S62.
23. Alizadeh AA, Gentles AJ, Alencar AJ, et al. Prediction of survival in diffuse large B-cell lymphoma based on the expression of 2 genes reflecting tumor and microenvironment. *Blood* 2011;118:1350-8.
24. Emura T, Chen YH. Gene selection for survival data under dependent censoring: A copula-based approach. *Stat Methods Med Res* 2016;25:2840-57.
25. Houdebine LM. Transgenic animal models in biomedical research. *Methods Mol Biol* 2007;360:163-202.
26. Lin S, Lin Y, Nery JR, et al. Comparison of the transcriptional landscapes between human and mouse tissues. *Proc Natl Acad Sci U S A* 2014;111:17224-9.
27. Jahan R, Ganguly K, Smith LM, et al. Trefoil factor(s) and CA19.9: A promising panel for early detection of pancreatic cancer. *EBioMedicine* 2019;42:375-85.
28. Hong X, Li ZX, Hou J, et al. Effects of ER-resident and secreted AGR2 on cell proliferation, migration, invasion, and survival in PANC-1 pancreatic cancer cells. *BMC Cancer* 2021;21:33.
29. Silva PM, da Silva IV, Sarmento MJ, et al. Aquaporin-3 and Aquaporin-5 Facilitate Migration and Cell-Cell Adhesion in Pancreatic Cancer by Modulating Cell Biomechanical Properties. *Cells* 2022;11:1308.
30. Zhang L, Lovell S, De Vita E, et al. A KLK6 Activity-Based Probe Reveals a Role for KLK6 Activity in Pancreatic Cancer Cell Invasion. *J Am Chem Soc* 2022;144:22493-504.
31. Khan S, Zafar N, Khan SS, et al. Clinical significance of MUC13 in pancreatic ductal adenocarcinoma. *HPB (Oxford)* 2018;20:563-72.
32. Wang X, Zhang CS, Dong XY, et al. Claudin 18.2 is a potential therapeutic target for zolbetuximab in pancreatic ductal adenocarcinoma. *World J Gastrointest Oncol* 2022;14:1252-64.
33. Ishikawa A, Sakamoto N, Honma R, et al. Annexin A10 is involved in the induction of pancreatic duodenal homeobox 1 in gastric cancer tissue, cells and organoids. *Oncol Rep* 2020;43:581-90.
34. Liu S, Cai Y, Changyong E, et al. Screening and Validation of Independent Predictors of Poor Survival in Pancreatic Cancer. *Pathol Oncol Res* 2021;27:1609868.
35. Gherardi E, Birchmeier W, Birchmeier C, et al. Targeting MET in cancer: rationale and progress. *Nat Rev Cancer* 2012;12:89-103.
36. Huang C, Liu H, Gong XL, et al. Expression of DNA methyltransferases and target microRNAs in human tissue samples related to sporadic colorectal cancer. *Oncol Rep* 2016;36:2705-14.

37. Jing W, Song N, Liu YP, et al. DNMT3a promotes proliferation by activating the STAT3 signaling pathway and depressing apoptosis in pancreatic cancer. *Cancer Manag Res* 2019;11:6379-96.
38. Wu C, Wu Z, Tian B. Five gene signatures were identified in the prediction of overall survival in resectable pancreatic cancer. *BMC Surg* 2020;20:207.
39. Li Z, Hu C, Yang Z, et al. Bioinformatic Analysis of Prognostic and Immune-Related Genes in Pancreatic Cancer. *Comput Math Methods Med* 2021;2021:5549298.
40. Li H, Hao C, Yang Q, et al. Identification of hub genes in chronic pancreatitis and analysis of association with pancreatic cancer via bioinformatic analysis. *Gen Physiol Biophys* 2022;41:15-30.
41. Logsdon CD, Simeone DM, Binkley C, et al. Molecular profiling of pancreatic adenocarcinoma and chronic pancreatitis identifies multiple genes differentially regulated in pancreatic cancer. *Cancer Res* 2003;63:2649-57.

Cite this article as: Zhou Y, Huang B, Zhang Q, Yu Y, Xiao J. Modeling of new markers for the diagnosis and prognosis of pancreatic cancer based on the transition from inflammation to cancer. *Transl Cancer Res* 2024;13(3):1425-1442. doi: 10.21037/tcr-23-1365